Appendix A. Extended Emissions Transport Analysis

To further investigate the transport of emissions from the fires identified in this demonstration for the June 26, 2020, exceptional event, an extended analysis was conducted to investigate emissions and transport of smoke from (1) fires more than 24 hours away based on trajectories, and (2) fires not identified in Section 3.2.1 with the traditional Q/d but where smoke transport to Clark County likely occurred. We analyzed the Rock Path and Miller Fires, and also considered a conservative estimate of emissions from the Twin Fire based on growth through approximately 4 p.m. PST on June 26. We refer to the resulting value calculated from additional fires as "Extended Q/d" to distinguish these results with the Q/d calculated in accordance with EPA guidance.

The total emissions from the fires were substantial on June 25 (**Table A-1**) and June 26 (**Table A-2**). These extended analyses provide evidence that additional fires (Rock Path and Miller fires) emitted ozone precursors in the days leading up to June 26, including on June 25, and that emissions transport from these fires and the Twin Fire contributed to the wildfire smoke event in Clark County, Nevada, on June 26.

Table A-1. Daily growth, emissions, and Extended Q/d for fires with potential smoke contribution on June 25, 2020. Growth was obtained from agency estimates available from the Incident Information System (InciWeb) and the Utah state fire information website. Column "E (Tons)" represents the sum of NO_x and Reactive VOC emissions. Aggregate Extended Q/d for the day was 0.5 tons/km.

Fire Name	Area (Acres)	Daily Growth (Acres)	NO_x (Tons)	VOCs (Tons)	Reactive VOCs (Tons)	E (Tons)	Distance (Km)	Extended Q/d (Tons/km)	Fuel Loading	Fire Size Data Source
Rock Path	9,000	9,000	35.33	185.66	111	147	325	0.5	Saltbrush shrubland	https://utahfireinfo.gov/2020/06/26/antelope-and-rock-path-update-6-26-2020/

Table A-2. Daily growth, emissions, and Extended Q/d for fires with potential smoke contribution on June 26, 2020. Growth was obtained from agency estimates available from the Incident Information System (InciWeb) and the Utah state fire information website. Column "E (Tons)" represents the sum of NO_x and Reactive VOC emissions. Aggregate Extended Q/d for the day was 2.5 tons/km.

Fire Name	Area (Acres)	Daily Growth (Acres)	NO_x (Tons)	VOCs (Tons)	Reactive VOCs (Tons)	E (Tons)	Distance (Km)	Extended Q/d (Tons/km)	Fuel Loading	Fire Size Data Source
Twin Fire	9,508	9,508	37.42	196.66	118	155	90	1.7	Creosote bush shrubland	https://inciweb.nwcg.gov/incident/6808/
Rock Path	20,117	11,117	43.64	229.33	138	181	325	0.6	Saltbrush shrubland	https://utahfireinfo.gov/2020/06/27/rock-path-fire-update-6-27-2020/
Miller Fire	1,847	1,847	13.35	357.3	214	228	250	0.9	Pinyon-Utah juniper woodland	https://inciweb.nwcg.gov/incident/6809/

Appendix B. Supporting Figures for Section 3.2.3 (Satellite Retrievals)

MODIS AOD images from MAIAC were inconclusive for the Rock Path, Miller, and Twin fires, but do not detract from our conceptual model because these fires do not show high enough AOD compared with other features in the southwestern U.S. to clearly distinguish them. These images are shown here for completeness.

MODIS AOD measurements indicate the concentration of light-absorbing aerosols, including those emitted by wildfires, in the total atmospheric column. Between June 23 and June 26, AOD measurements show that aerosols over southern Nevada are not enhanced (**Figure B-1**). Zooming in over Clark County, we find that aerosols in the Clark County area are not enhanced on June 26 (**Figure B-2**), although cloud cover may have obscured data collection. AOD from MODIS does not provide strong evidence for or against smoke impacts in Clark County on June 26.

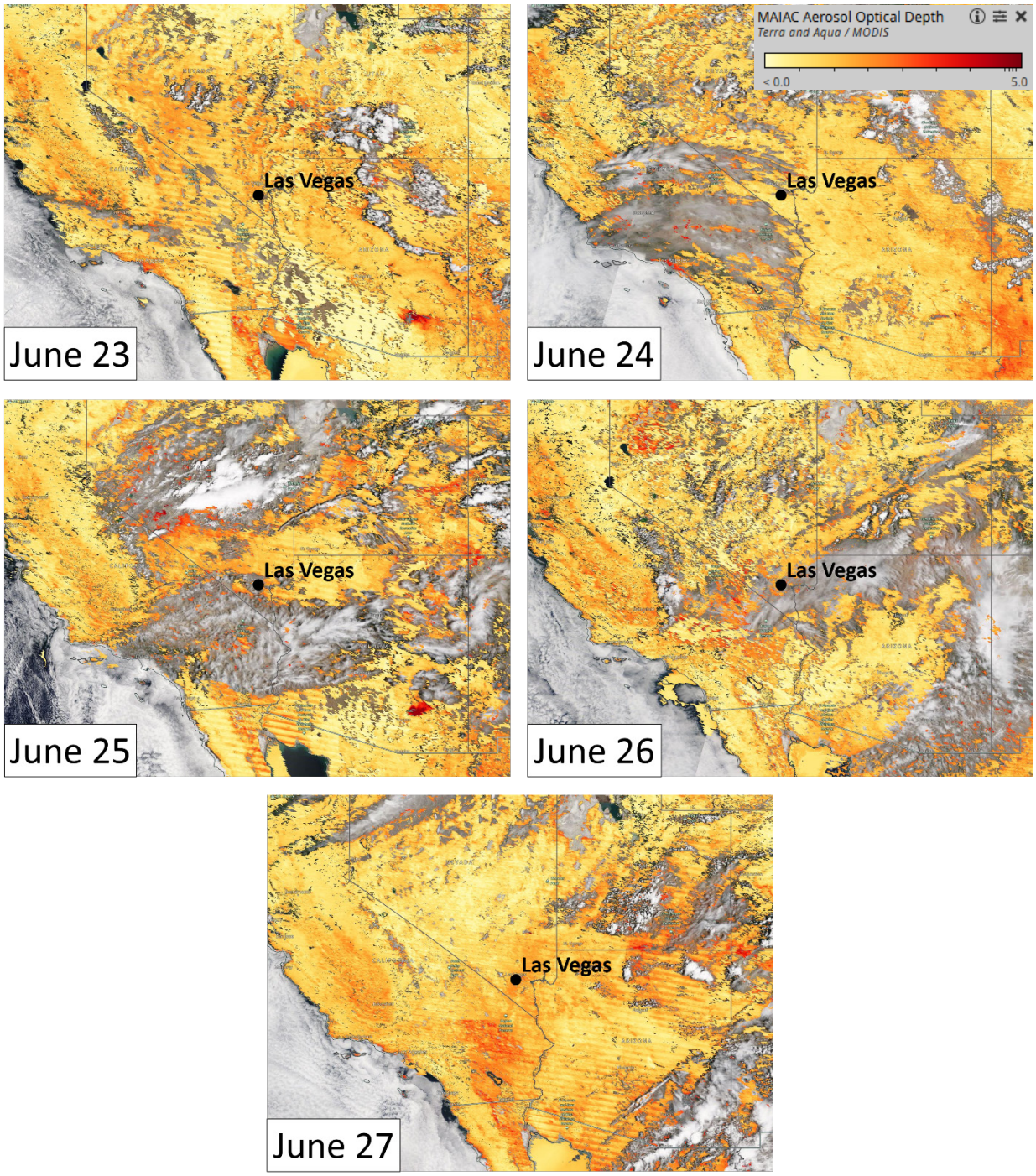

Figure B-1. MAIAC MODIS Aqua/Terra combined AOD retrievals June 23 – 27, covering the three days before the exceptional event, the day of the event (June 26), and the day after the event. AOD color ranges from yellow (low AOD) to red (high AOD).

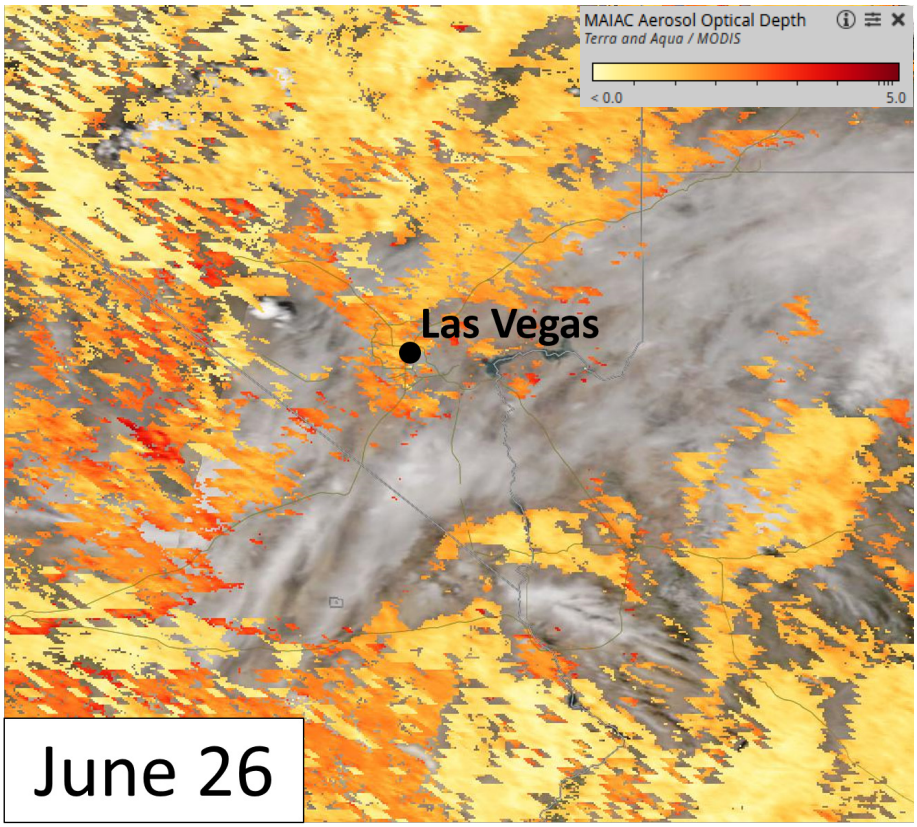

Figure B-2. A zoomed-in view of Clark County from the MAIAC MODIS Aqua/Terra combined AOD retrieval during the exceptional event on June 26, 2020.

Appendix C. Supporting Figures for Section 3.2.4 (Supporting Pollutant Trends)

Observations of NO_x ($NO + NO_2$) are unavailable from exceedance-affected Paul Meyer monitoring site. **Figure C-1** shows observations during the event period at the Joe Neal and Jerome Mack sites, the only two monitoring sites in Clark County for which NO_x data is available. NO_x concentrations during the event period at these supporting sites did not deviate significantly from diurnal profiles. Though concentrations of NO_x at the Joe Neal and Jerome Mack sites can provide a view of any regional abnormalities, this data should not be used as a direct proxy for concentrations at Paul Meyer due to local variation.

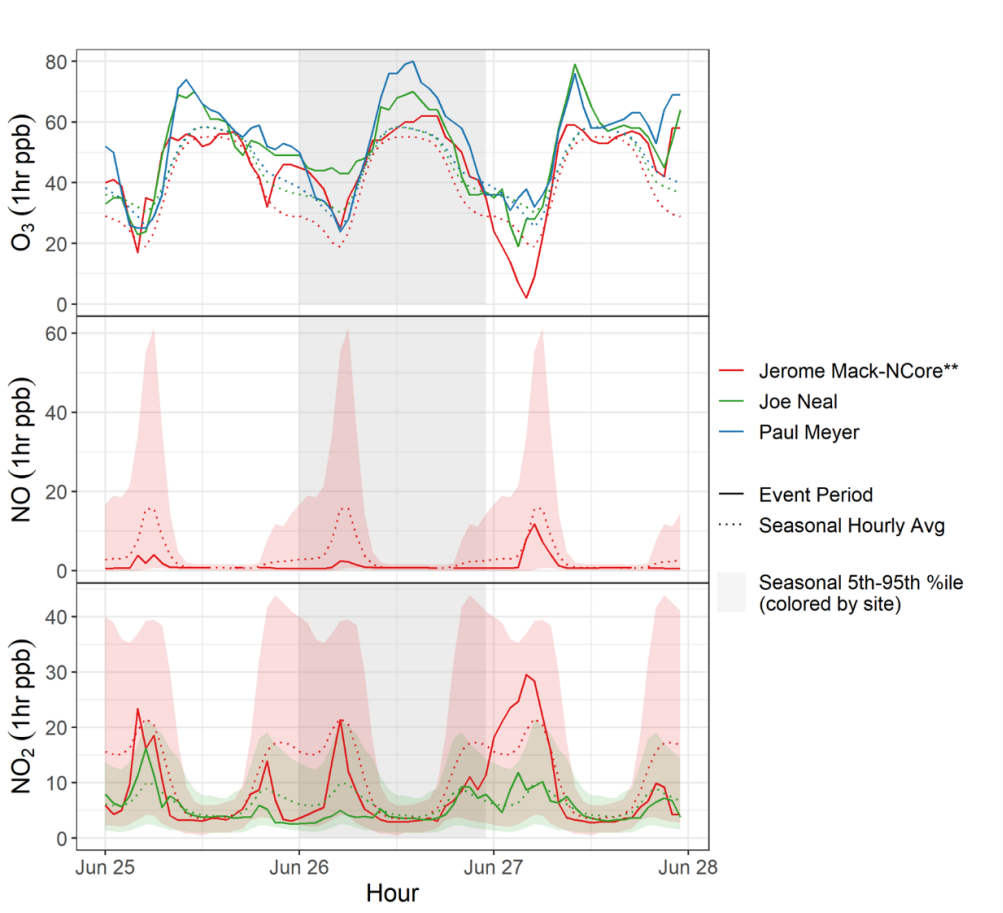

Figure C-1. Ozone and NO_x concentrations during the June 26 exceptional event. The top figure shows ozone concentrations from all sites on June 25-28 (solid lines) and five-year seasonal averages (May–Sept.) for each site (dotted lines). The middle plot shows NO concentrations on June 26 (solid line), the seasonal average (dotted line), and the seasonal 5th to 95th percentile (shaded area) for select sites with NO measurements. The bottom plot shows the same information as the middle plot, but for NO_2. 5 years of NO data is available from the Jerome Mack site, and 4 and 5 years of NO_2 data is available from the Jerome Mack and Joe Neal sites, respectively.

OC/EC data from Las Vegas was inconclusive for the June 26 wildfires, but did not detract from our conceptual model because overall OC/EC ratios increasing up to the EE date could indicate wildfire influence.

Speciation of $PM_{2.5}$ can provide further evidence of smoke impact in a region. The ratio of $PM_{2.5}$ organic carbon (OC) to $PM_{2.5}$ elemental carbon (EC) has been used to differentiate combustion sources of biomass burning from mobile sources. Biomass burning results in a higher OC/EC ratio (7.0-15.0) (Lee et al., 2005; Pio et al., 2008) than gasoline (3.0-4.0) or diesel vehicles (<1.0) (Lee and Russell, 2007; Zheng et al., 2007). This is, however, complicated by mixing and photochemistry within Clark County. $PM_{2.5}$ speciation data is available in Clark County every three days. **Figure C-2** displays a time series of the OC to EC ratio (blue line) throughout the event period. June 26 is marked by a

dotted gray line. Although the ratio of OC to EC showed an increasing trend from June 23 to June 26 and 29, OC/EC values were ≤4 before and on the event date, indicating that this analysis could not definitely detect a biomass burning signature. The OC/EC ratio of ambient $PM_{2.5}$ could be modified from the OC/EC emission ratio of fresh smoke and is not necessarily conserved during transport of smoke plumes to Clark County. However, this result does not rule out the contribution of biomass burning, as detailed in the additional analyses in this section.

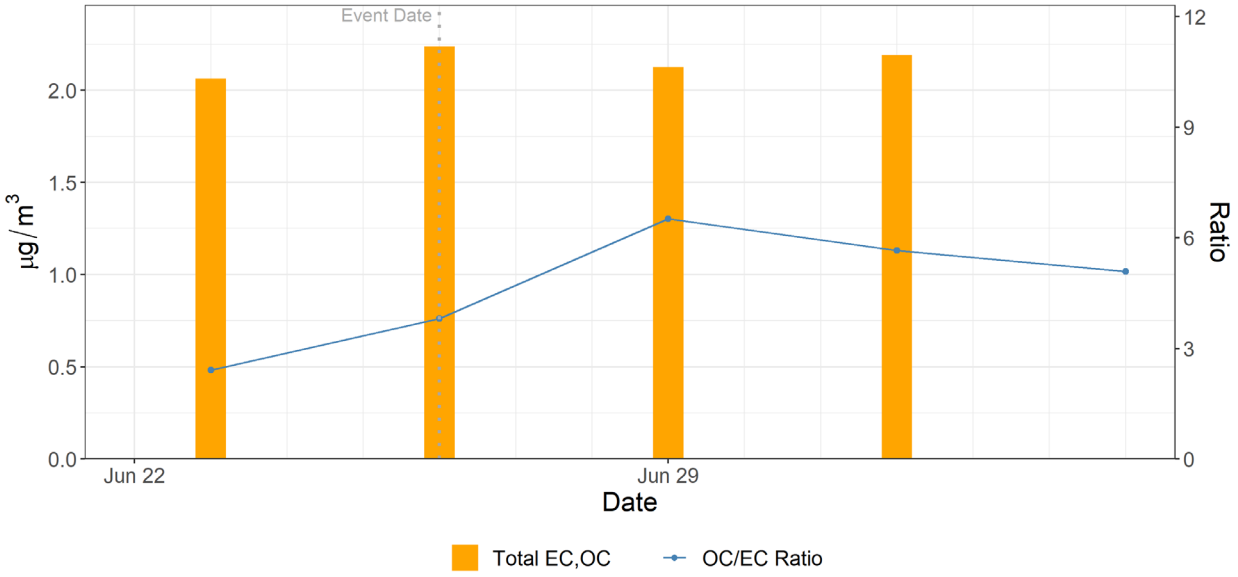

Figure C-2. A timeseries of the ratio of $PM_{2.5}$ organic carbon (OC) to elemental carbon (EC) (blue line) in Clark County during the June 26 event period. Higher OC/EC ratios result from biomass burning (7.0-15.0) (Lee et al., 2005; Pio et al., 2008) than gasoline (3.0-4.0) or diesel vehicles (<1.0).

References

Lee S., Baumann K., Schauer J.J., Sheesley R.J., Naeher L.P., Meinardi S., Blake D.R., Edgerton E.S., Russell A.G., and Clements M. (2005) Gaseous and particulate emissions from prescribed burning in Georgia. *Environ. Sci. Technol.*, 39(23), 9049-9056, doi: 10.1021/es051583l, December 1.

Lee S. and Russell A.G. (2007) Estimating uncertainties and uncertainty contributors of CMB PM2.5 source apportionment results. Atmospheric Environment, 41(40), 9616-9624, 2007/12/01/. Available at https://www.sciencedirect.com/science/article/pii/S1352231007007406.

Pio C.A., Legrand M., Alves C.A., Oliveira T., Afonso J., Caseiro A., Puxbaum H., Sanchez-Ochoa A., and Gelencser A. (2008) Chemical composition of atmospheric aerosols during the 2003 summer intense forest fire period. Atmospheric Environment, 42, 7530-7543.

Zheng M., Cass G.R., Ke L., Wang F., Schauer J.J., Edgerton E.S., and Russell A.G. (2007) Source apportionment of daily fine particulate matter at Jefferson Street, Atlanta, GA, during summer and winter. J. Air Waste Manage., 57(2), 228-242, 2007/02/01. Available at https://doi.org/10.1080/10473289.2007.10465322.

Appendix D. Supporting Figures for Section 3.3.1 (Total Column Measurements)

The Cloud-Aerosol Light Detection and Ranging (LIDAR) and Infrared Pathfinder Satellite Observation (CALIPSO) data were inconclusive for both the Clark County area and the Nevada/Utah fires on June 26, 2020, because the satellite overpass was too far west. This section provides the nearest overpass on June 26, but this data does not provide evidence for or against the June 26 exceptional event.

The CALIPSO system is a remote sensing instrument mounted on the CloudSat satellite that provides vertical profile measurements of atmospheric aerosols and clouds. Detected aerosols are classified into marine, marine mixture, dust, dust mixture, clean/background, polluted continental, smoke, and volcanic aerosol types.

The most relevant CALIPSO aerosol retrieval over Clark County for the June 26 ozone event is available at approximately 2:40 a.m. local time on June 26 (**Figures D-1 and D-2**). Unfortunately, the CALIPSO vertical profile does not capture information directly over Clark County during the event; it does, however, provide information about the column above areas to the west of Clark County in western Nevada and southern California. Increased backscatter between the altitudes of approximately 1,000 to 3,000 m provides evidence of increased aerosols at low levels in the vertical columns near Clark County (**Figure D-3**). Additionally, CALIPSO classifies this aerosol as polluted dust, but corroborating evidence from HMS smoke and other satellite retrievals indicates that it is possibly smoke (**Figure D-4**).

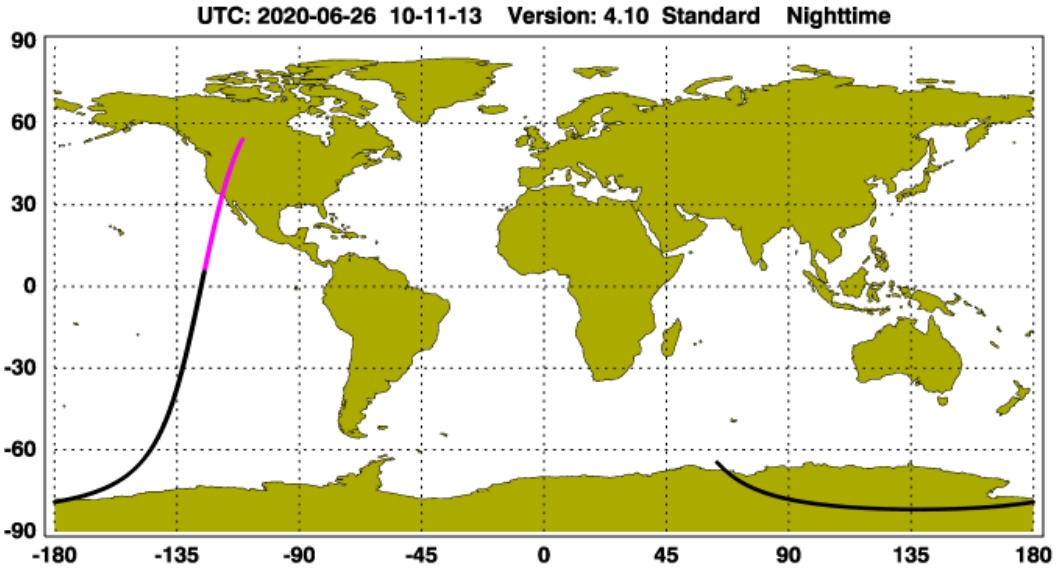

Figure D-1. The CALIPSO retrieval path for June 26, 2020. This overpass was the closest to the Rock Path, Miller, and Twin fires and Clark County and the nearest in time.

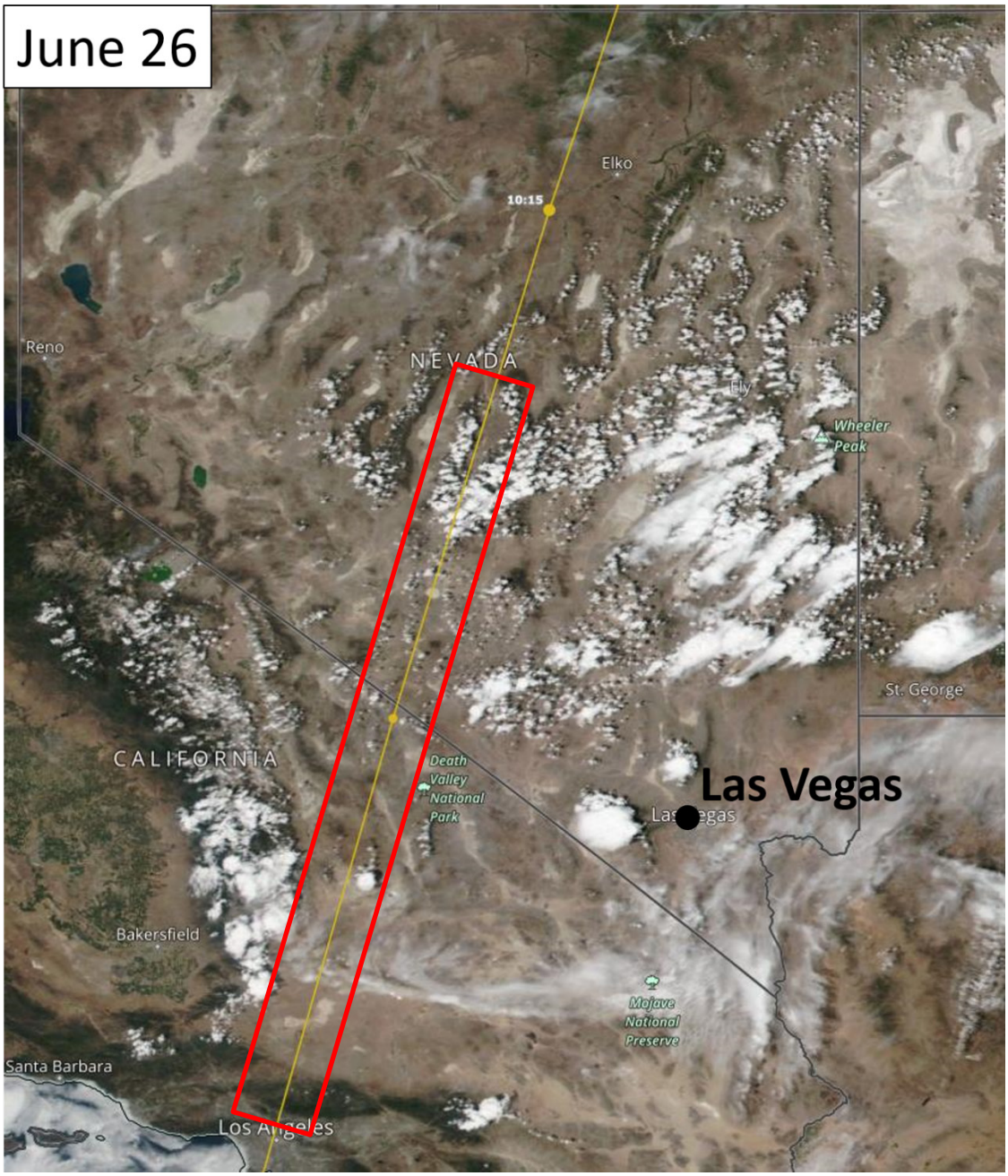

Figure D-2. The CALIPSO retrieval path for June 26, 2020. This overpass was the closest to the Rock Path, Miller, and Twin fires and Clark County and the nearest in time.

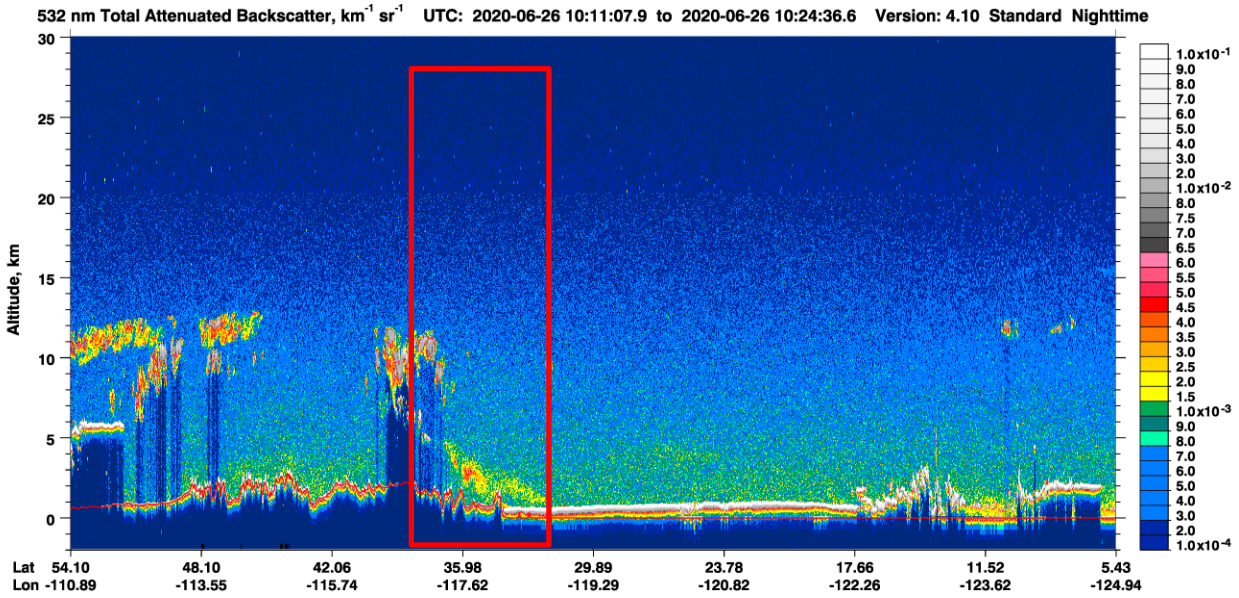

Figure D-3. CALIPSO total column profile backscatter information for the June 26, 2020, overpass west of the Rock Path, Miller, and Twin fires and Clark County (approximate areas indicated by a red box).

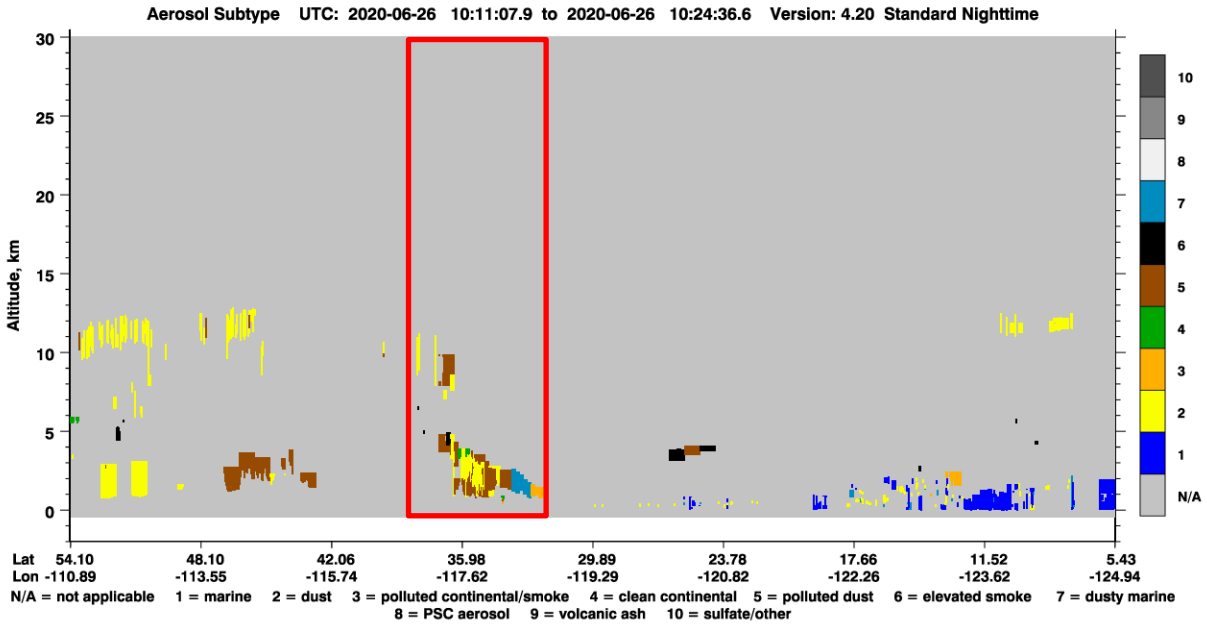

Figure D-4. CALIPSO total column profile aerosol subtype information for the June 26, 2020, overpass west of the Rock Path, Miller, and Twin fires and Clark County (approximate areas indicated by a red box).

Appendix E. Supporting Figures and Tables for Section 3.3.2 (Matching Day Analysis

Identification of matching (meteorologically similar) days includes a comparison of meteorology maps between June 26, 2020, and each date subset from candidate matching days. The surface maps for June 26, and each date listed in Table 3-12 in Section 3.3.2 all show a surface low pressure system directly over Clark County, and most dates have an area of high pressure directly to the east. Surface maps for June 26, 2020, and each date in Table 3-12 are shown in **Figure E-1 through E-8**. Each upper-level map shows a very low gradient of height contours over the region. 500 mb maps for June 26, 2020, and each date in Table 3-12 are shown in **Figure E-9 through E-16**.

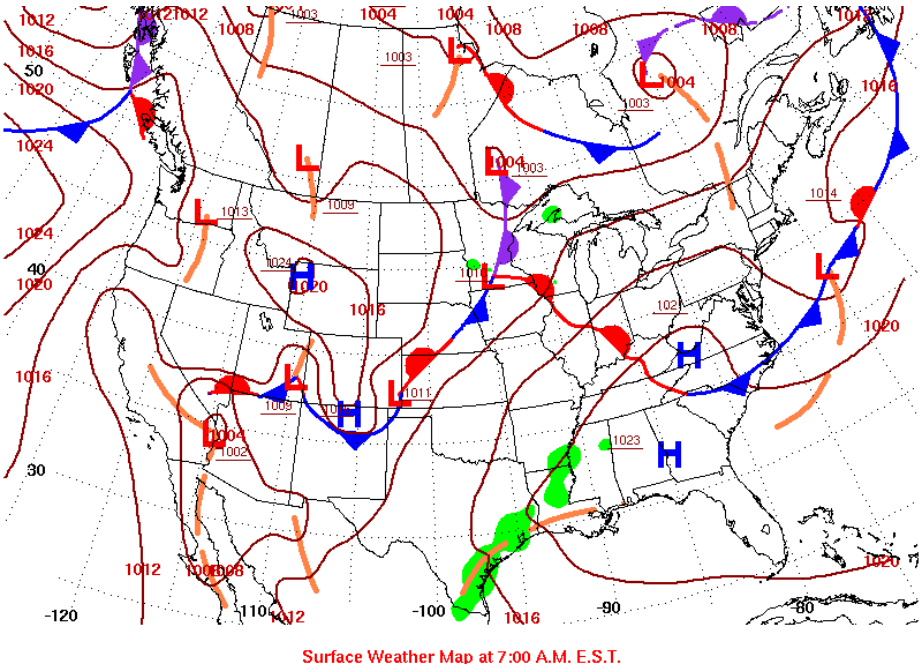

Figure E-1. Surface meteorology map on June 26, 2020 (the event date).

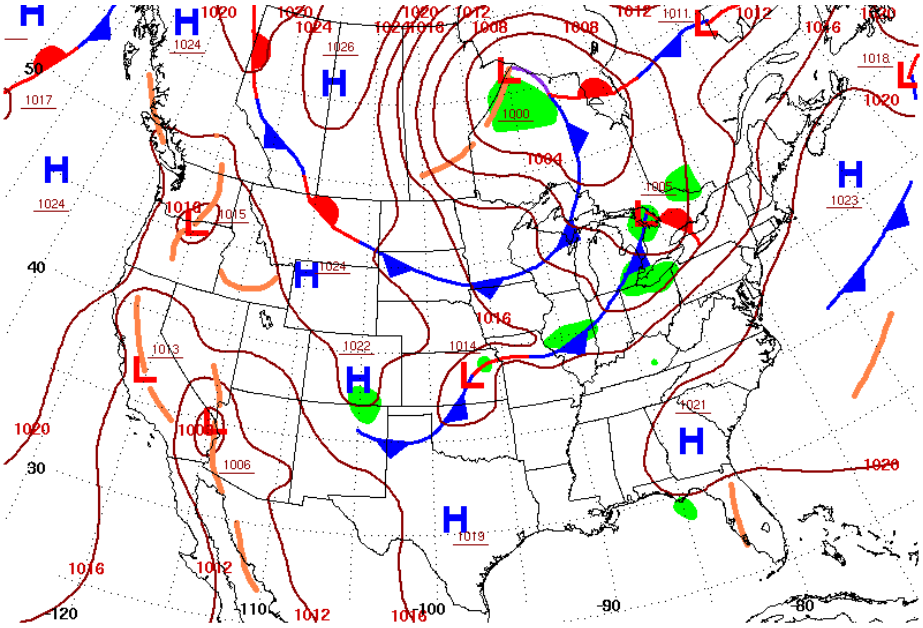

Figure E-2. Surface meteorology map on July 13, 2014.

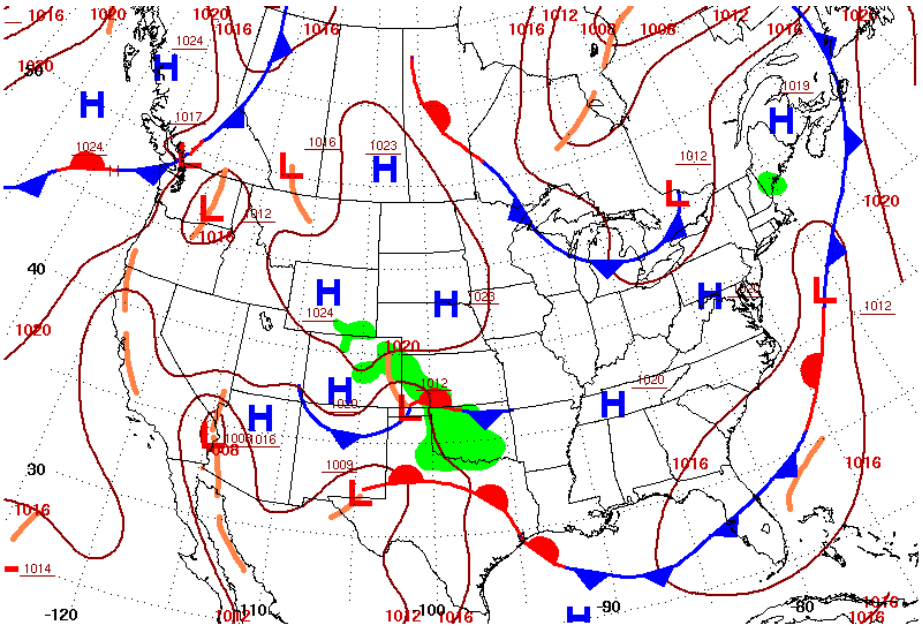

Figure E-3. Surface meteorology map on July 30, 2014.

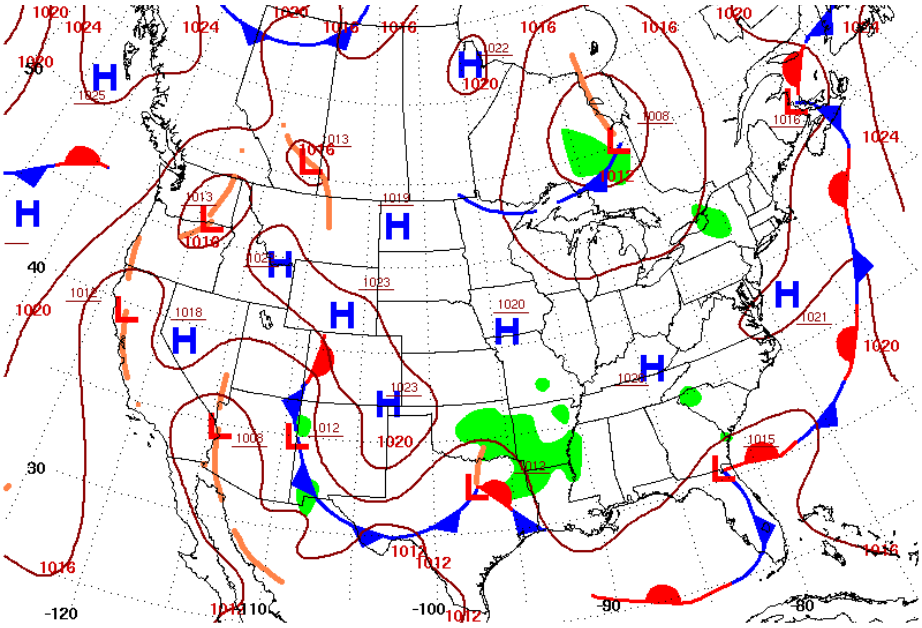

Figure E-4. Surface meteorology map on July 31, 2014.

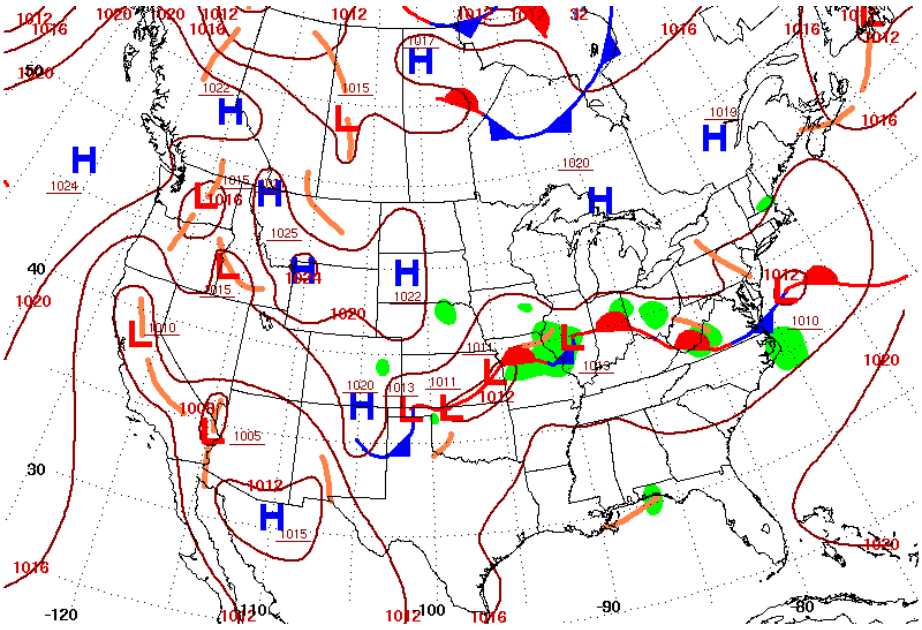

Figure E-5. Surface meteorology map on June 26, 2015.

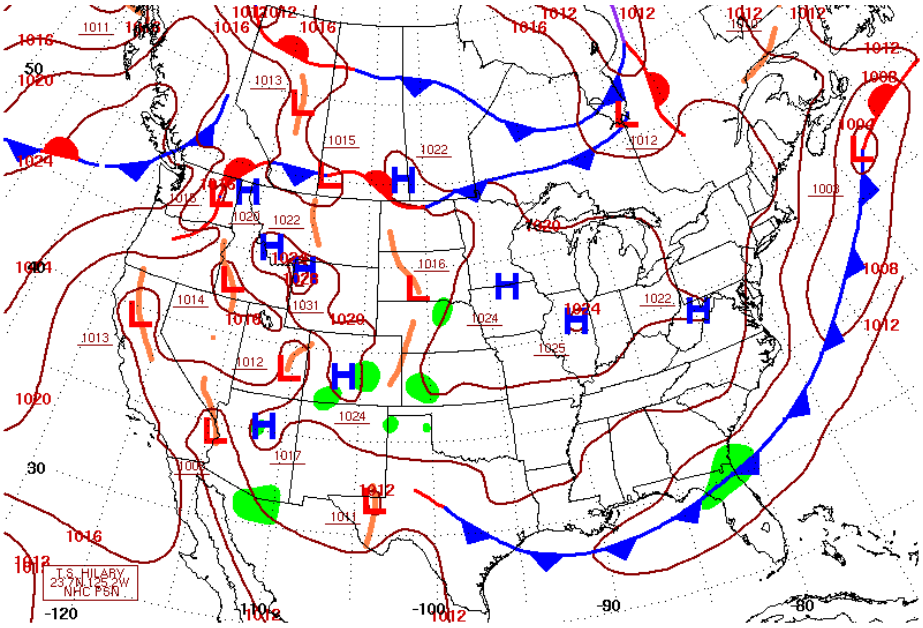

Figure E-6. Surface meteorology map on July 30, 2017.

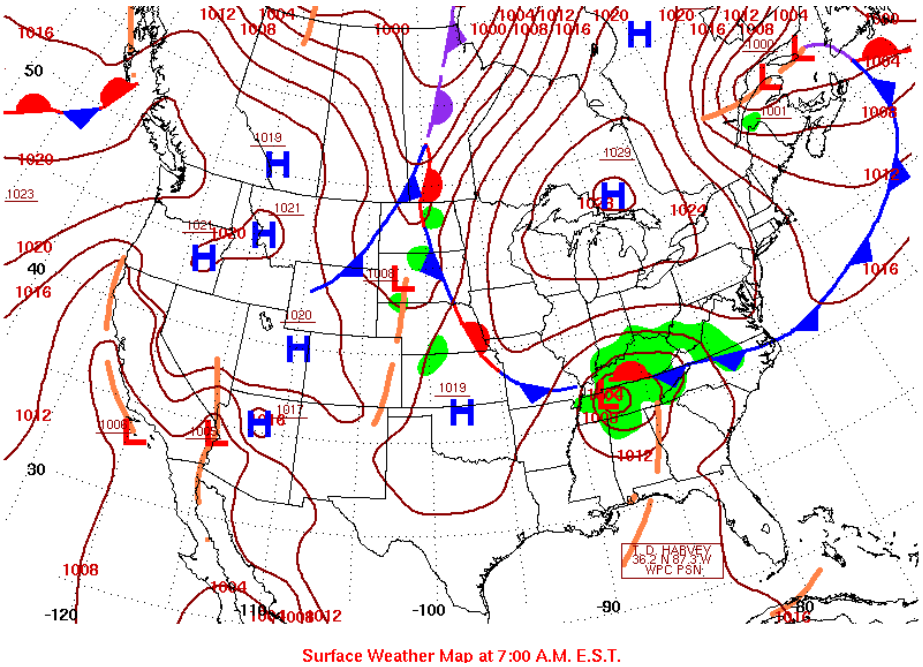

Figure E-7. Surface meteorology map on September 1, 2017.

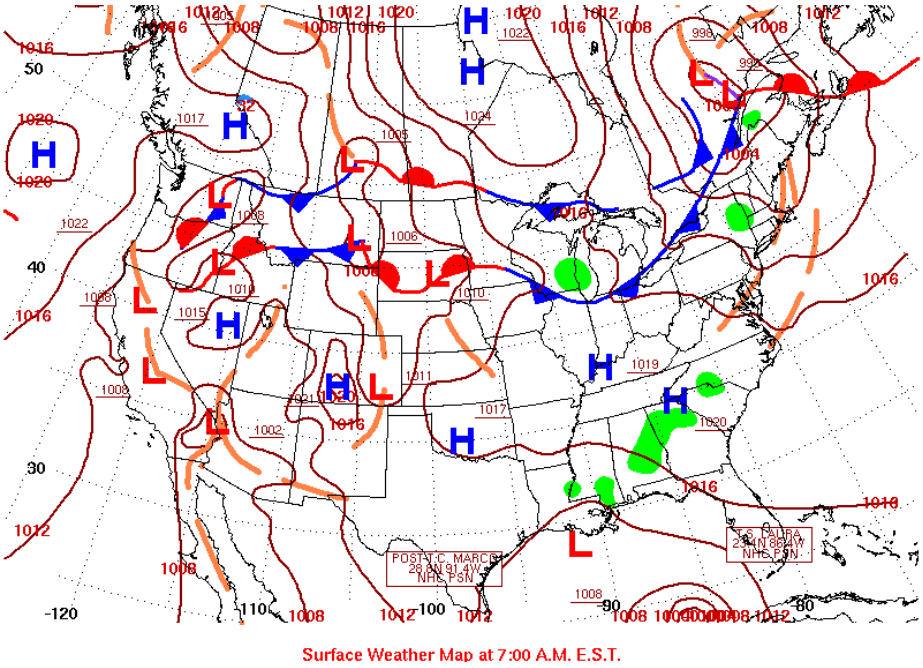

Figure E-8. Surface meteorology map on August 25, 2020

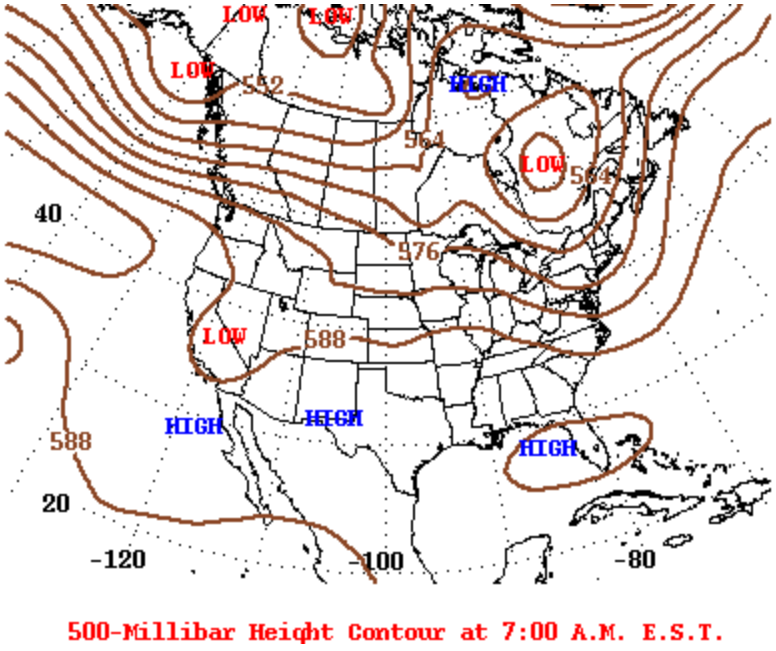

Figure E-9. 500 mb meteorology map on June 26, 2020 (the event date).

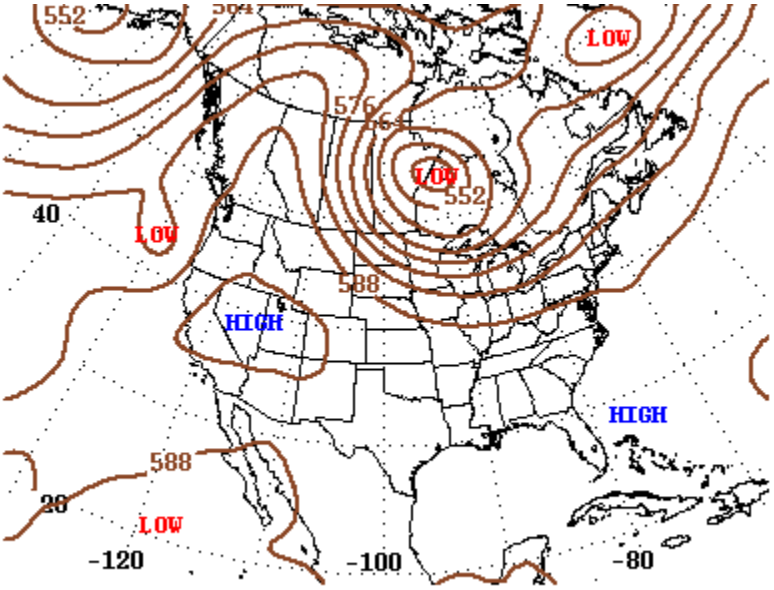

Figure E-10. 500 mb meteorology map on July 13, 2014.

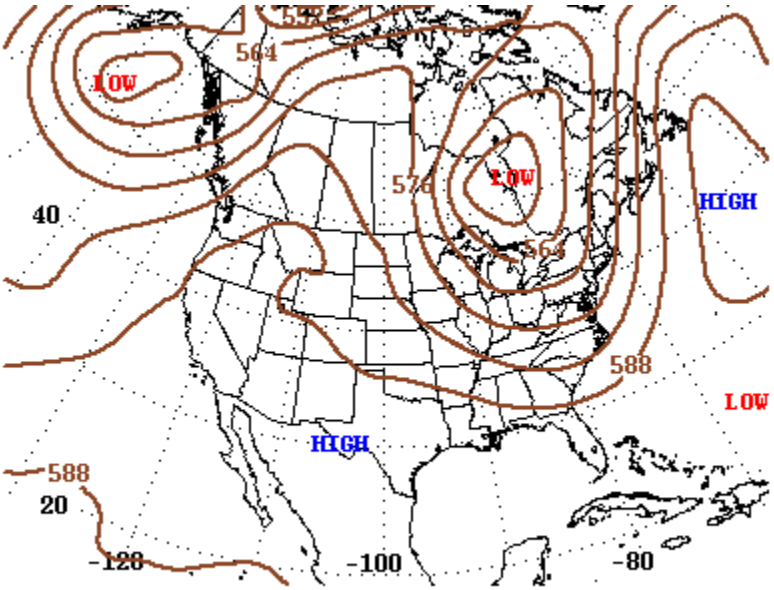

Figure E-11. 500 mb meteorology map on July 30, 2014.

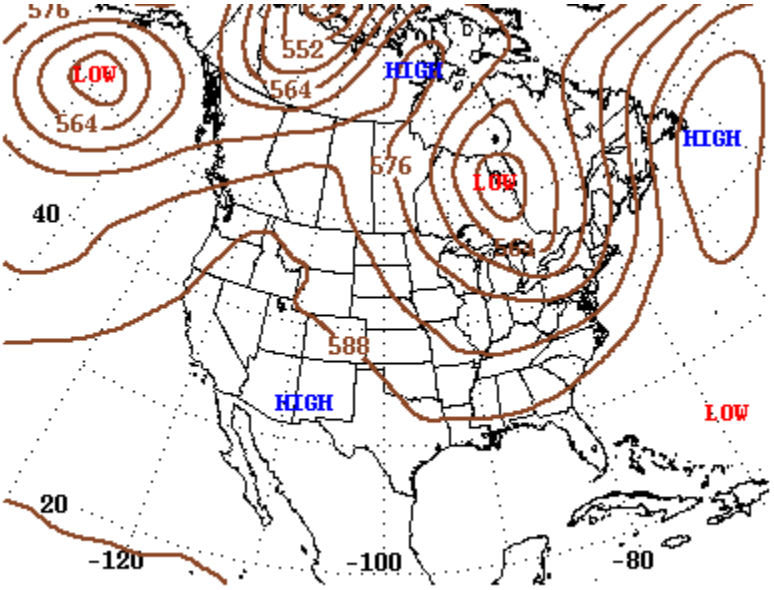

Figure E-12. 500 mb meteorology map on July 31, 2014.

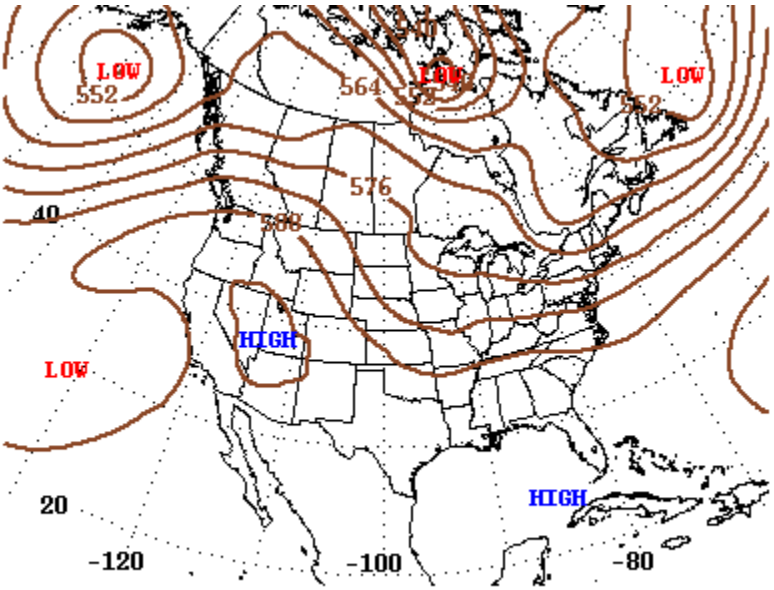

Figure E-13. 500 mb meteorology map on June 26, 2015.

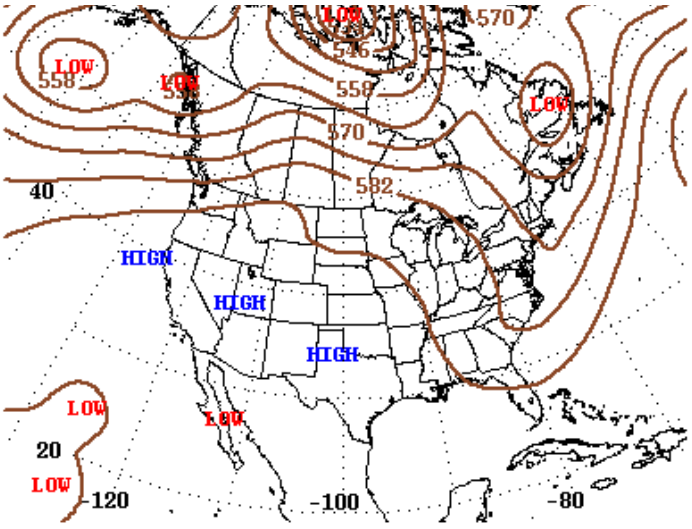

Figure E-14. 500 mb meteorology map on July 30, 2017.

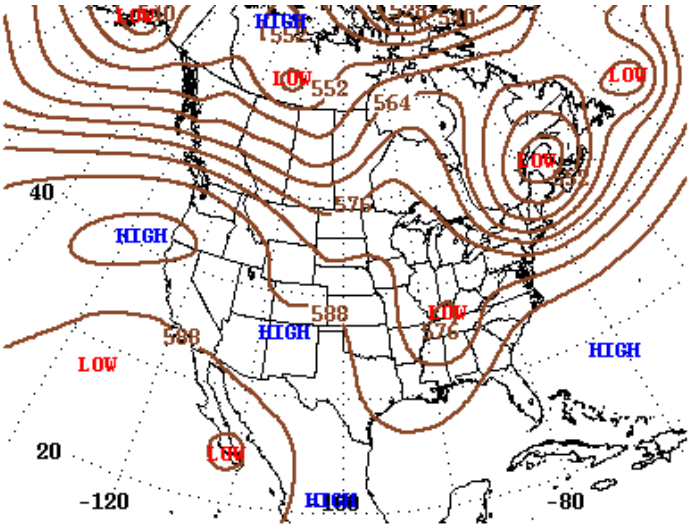

Figure E-15. 500 mb meteorology map on September 1, 2017.

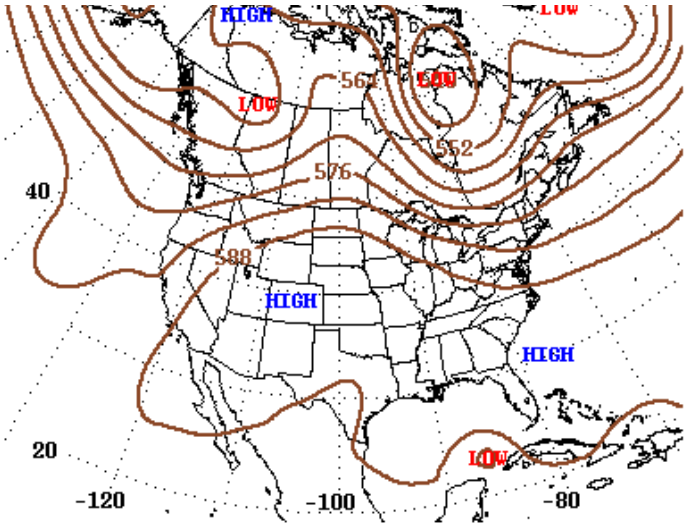

Figure E-16. 500 mb meteorology map on August 25, 2020.

Appendix F. GAM Residual Histograms and Scatter Plots from Concurred Exceptional Event Demonstrations

The following are GAM residual histograms and scatter plots from the concurred Arizona Department of Environmental Quality demonstration (Arizona Department of Environmental Quality 2016) and the submitted Texas Commission on Environmental Quality demonstration (Texas Commission on Environmental Quality 2021) for comparison with our GAM residual analysis. The figures in this Appendix show the good residual results from concurred and currently submitted exceptional events demonstrations to which we compared our results. Based on this comparison, we suggest that our GAM results show a well-fit, unbiased model. A well-fit GAM model should show a normal distribution of residuals at all sites modeled (ADEQ example in **Figure F-1**) and show no pattern or bias between GAM residuals and predicted values (TCEQ example in **Figure F-2**). These figures compare well with our GAM results in Section 3.3.3 of the main report.

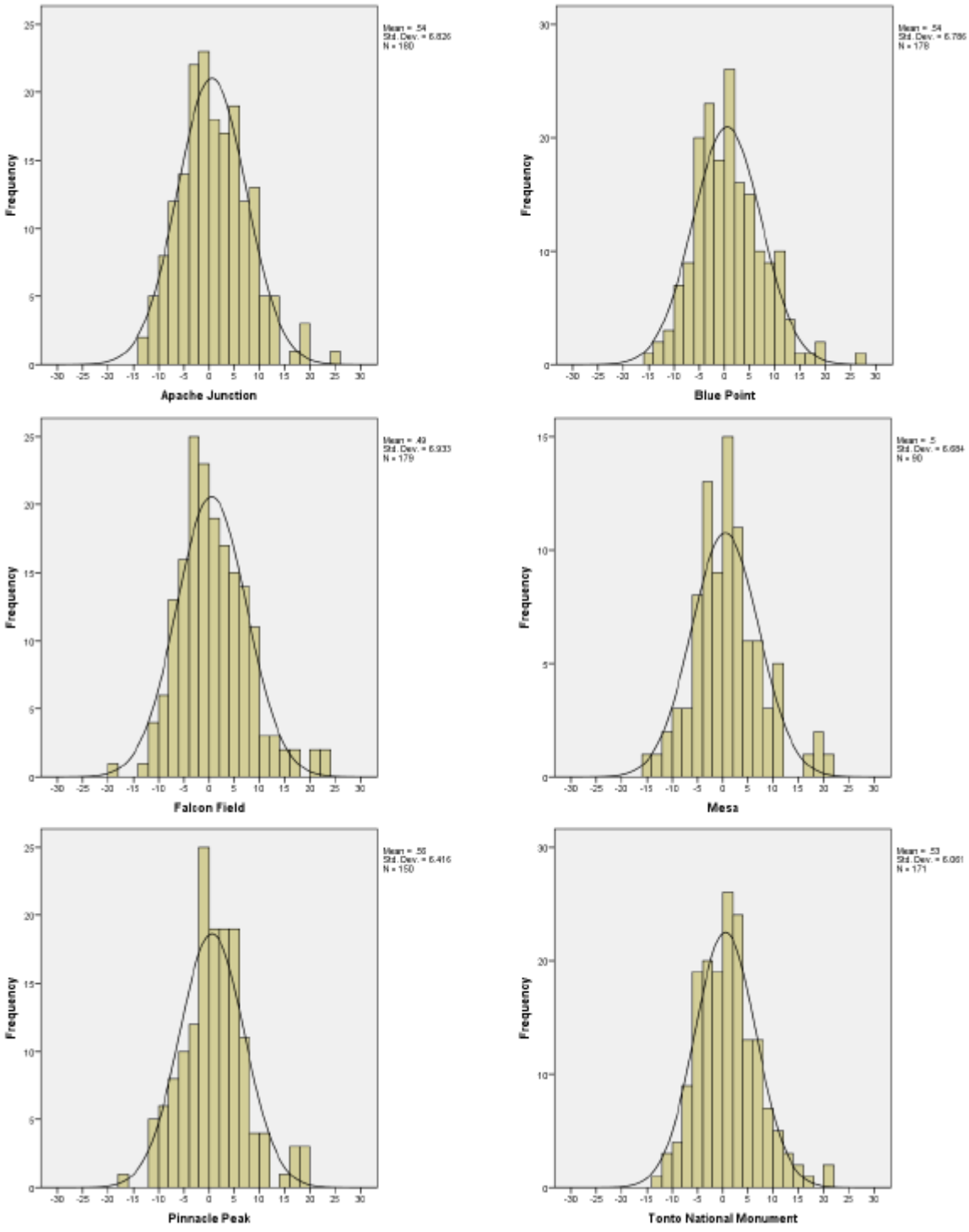

Figure F-1. Histograms of residuals results at each monitoring site from the Arizona DEQ GAM Analysis (Arizona Department of Environmental Quality 2016).

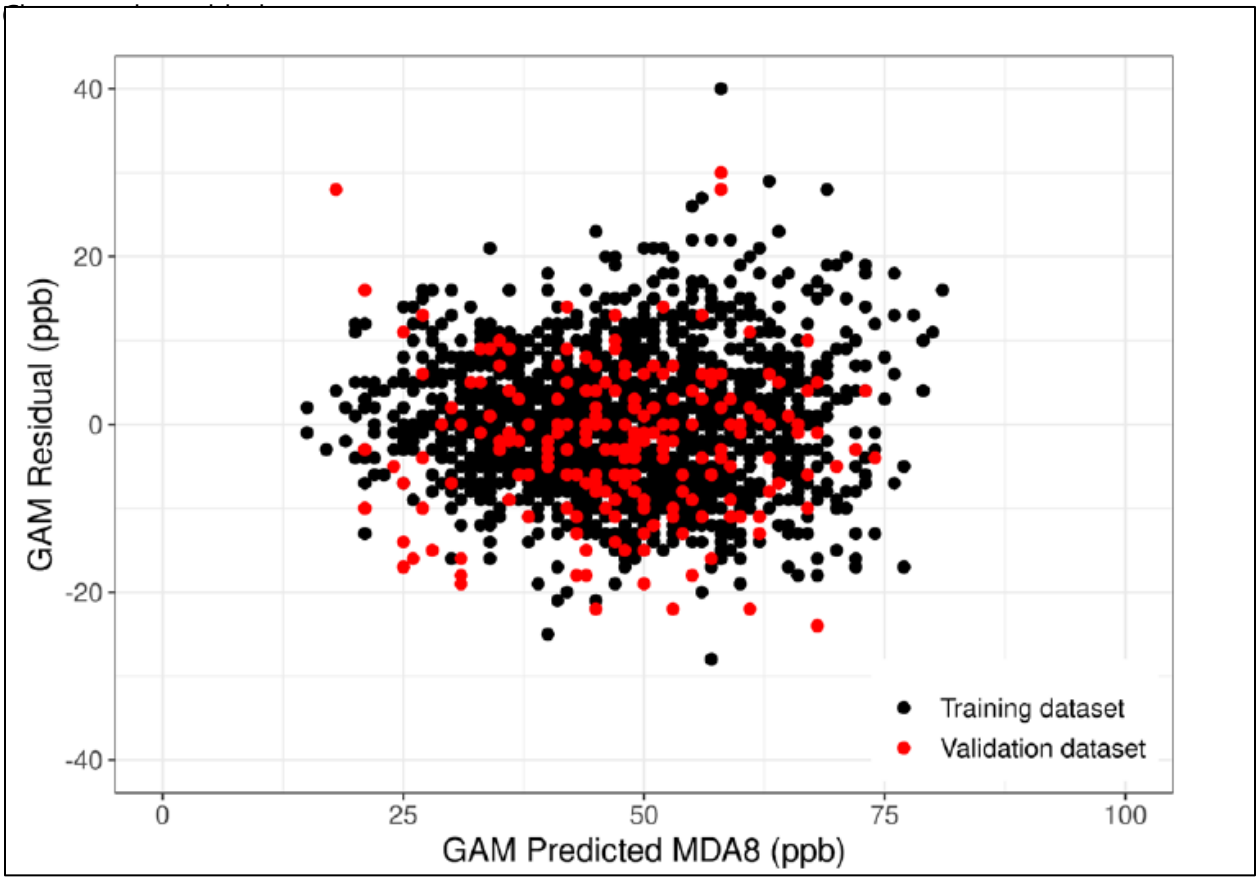

Figure F-2. Scatter plot of GAM residuals (observed – GAM predicted MDA8 ozone) vs. GAM predicted MDA8 ozone from the TCEQ submitted GAM analysis. Training data is shown in black and validation data is shown in red (Texas Commission on Environmental Quality 2021).

References

Arizona Department of Environmental Quality (2016) State of Arizona exceptional event documentation for wildfire-caused ozone exceedances on June 20, 2015 in the Maricopa nonattainment area. Final report, September. Available at https://static.azdeq.gov/pn/1609_ee_report.pdf.

Texas Commission on Environmental Quality (2021) Dallas-Fort Worth area exceptional event demonstration for ozone on August 16, 17, and 21, 2020. April. Available at https://www.tceq.texas.gov/assets/public/airquality/airmod/docs/ozoneExceptionalEvent/2020-DFW-EE-Ozone.pdf.

Appendix G. Analysis of COVID Restrictions on Ozone

Mobile emission sources decreased throughout the U.S. during the mobility restrictions for the COVID-19 pandemic beginning in mid-March 2020. Because decreases in nitrogen oxides (NO_x) emissions from mobile sources could result in higher ozone concentrations, we evaluated the potential contribution and sensitivity of the COVID-19 shutdown effects on ozone concentrations and MDA8 ozone on exceptional event (EE) days. Ozone production has non-linear dependence on precursor emissions of NO_x and volatile organic compounds (VOCs), as well as meteorological conditions. Changes in precursors also shift photochemical regimes. Thus, the effects of COVID-induced NO_x emission changes on ozone are complex and uncertain (Kroll et al., 2020). Recent studies have found variable ozone responses during lockdowns across countries, with responses ranging from −2 to +10% (Venter et al., 2020). Park et al., 2020 found spatially disparate effects of higher ozone concentrations downwind of Los Angeles and lower concentrations in the western LA basin. To evaluate the potential influence of COVID-19 shutdown precursor emission decreases or increases in MDA8 ozone, we compared ozone concentrations in May 2020 to the historical climatology, and compared the GAM residuals from May 2020 with those for the same historical record.

Based on 2017 emission inventories in Las Vegas, on-road mobile sources comprise 40% of NO_x emissions and total mobile (vehicle + aviation) emissions comprise 88% of total NO_x emissions for typical ozone season weekday (SIP Plan Revision, Clark County 2015). In contrast, only 11% of VOC emissions originate from on-road mobile sources. The effects of decreased mobility due to COVID restrictions has a significant effect on total NOx emissions, but minimal effect on VOC emissions. To determine the time period for these effects, we compared 2020 daily traffic count data from the Nevada Department of Transportation with that from 2019 at 10 monitoring sites (two examples in Figure G-1). On-road traffic activity was significantly reduced from mid-March through early-June 2020 in Clark County compared with 2019 (Figure G-1). Although aviation activity remained lower than pre-pandemic levels for a longer duration of 2020, commercial aviation represents only 12% of NO_x emissions in Clark County. Thus, the reduced aviation activity had a minimal influence on the precursors available for ozone formation from mid-June 2020 onwards. In this section, we focus on May 2020, the first month of 2020 with EE days.

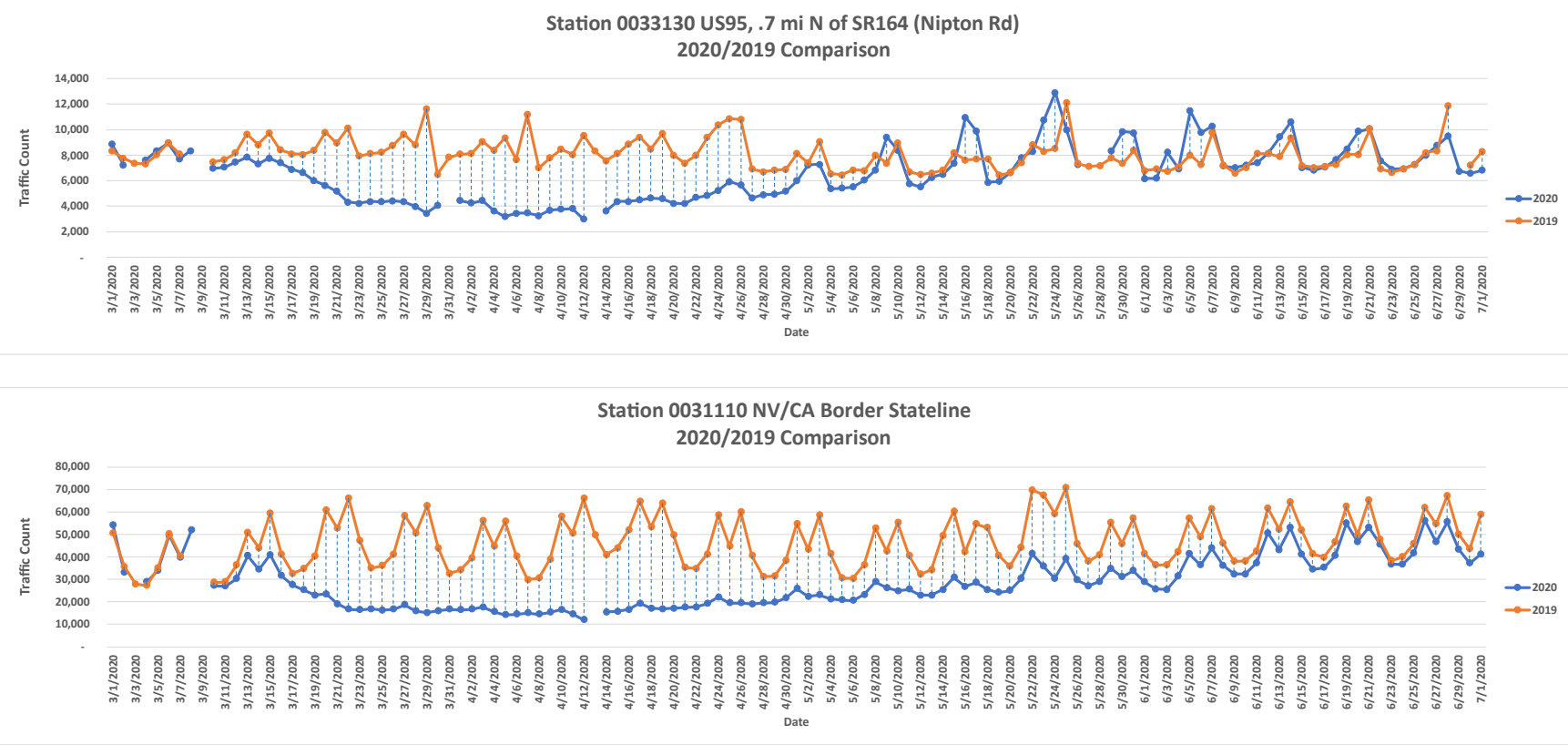

Figure G-1. Time series of 2020 and 2019 traffic counts at two stations: (top) US95, south of Las Vegas, and (bottom) at the Nevada-California border, west of Las Vegas. Data were provided by the Nevada Department of Transportation.

We performed two sub-analyses for the ozone comparison to historical climatology. First, we compared the distribution of daily MDA8 ozone during May 2020 with those during May in each of the previous 5 years. Across all EE sites, we found median 2020 MDA8 ozone was not statistically different than any of the previous five years illustrated by the overlap in the 95th confidence intervals of the monthly medians in previous years with that for 2020 (**Figure G-2**). Furthermore, monthly median MDA8 ozone during May 2020 was not particularly high (much less than 65 ppb) at all sites despite the exceptional event days. This indicates that the EE day exceedances were extreme episodes that did not affect the monthly median. Thus, the observations do not suggest a month-long high ozone effect due to COVID emission precursor changes. Second, we compared the historical distribution of daily MDA8 ozone during May with the observations during May 2020 (**Figure G-3**). Across all EE sites, MDA8 ozone on the exceedance days for a given site rank above the confidence interval of the historical daily median MDA8 ozone. Based on these sub-analyses, we conclude that although precursor NO_x emissions decreased during May 2020 due to COVID restrictions, MDA8 ozone concentrations were not statistically higher than previous years. Therefore, the EE days cannot be attributed to a consistent COVID-shutdown influenced month-long increase in ozone concentrations.

To evaluate the GAM model residuals during the COVID shutdown period, Figure 3-37 in Section 3.3.3 provides a more in-depth look at results from April and May 2020, which are the most heavily affected months of the shutdown/COVID restrictions. The 95th confidence interval of the median GAM MDA8 residuals (shown by the notches in the box plots) overlap between 2020 and most other years, except for 2015 and 2016. The May 2020 median residual with EE days (1.5 ppb) is within the typical GAM model uncertainty (+/- [CI from Figure 3-31 in Section 3.3.3]). This analysis shows that the median GAM residuals during May 2020 were within the typical GAM model error during the previous 5 years.

In summary, although mobile source precursor emissions of NO_x decreased during April and May 2020 due to COVID shutdown restrictions, we did not observe statistically higher ozone concentrations, nor a higher residual in the GAM model, during May 2020. We find consistent evidence across analyses that the EE day ozone concentrations cannot be attributed to an increase in ozone concentrations associated with COVID shutdown periods.

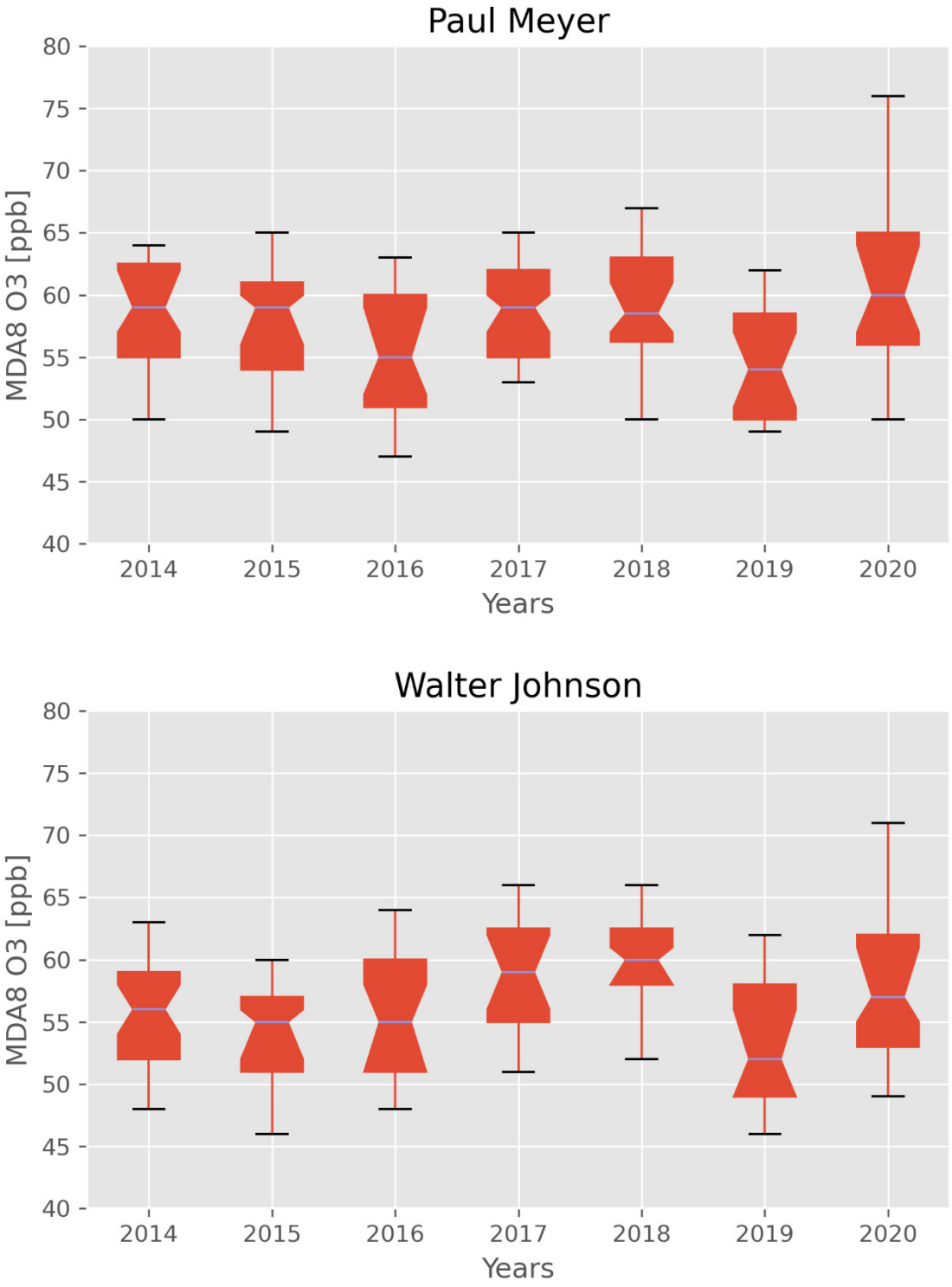

Figure G-2. Annual May distributions of MDA8 ozone at sites with exceptional events during May 2020. Notches denote 95th confidence interval of the median, boxes are 25th, 50th and 75th percentiles, and whiskers are 5th and 95th percentiles.

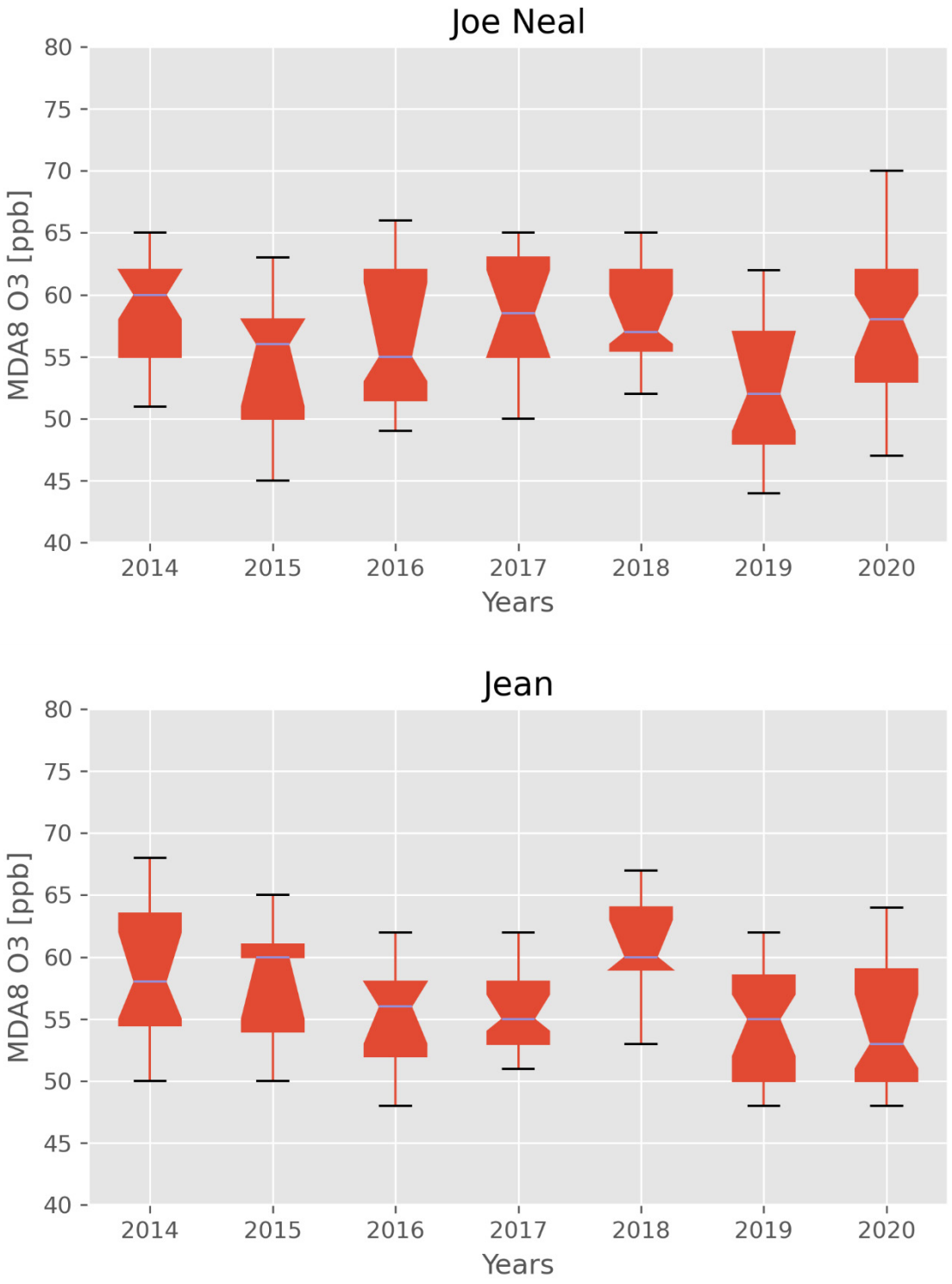

Figure G-2 (Cont.). Annual May distributions of MDA8 ozone at sites with exceptional events during May 2020. Notches denote 95th confidence interval of the median, boxes are 25th, 50th and 75th percentiles, and whiskers are 5th and 95th percentiles.

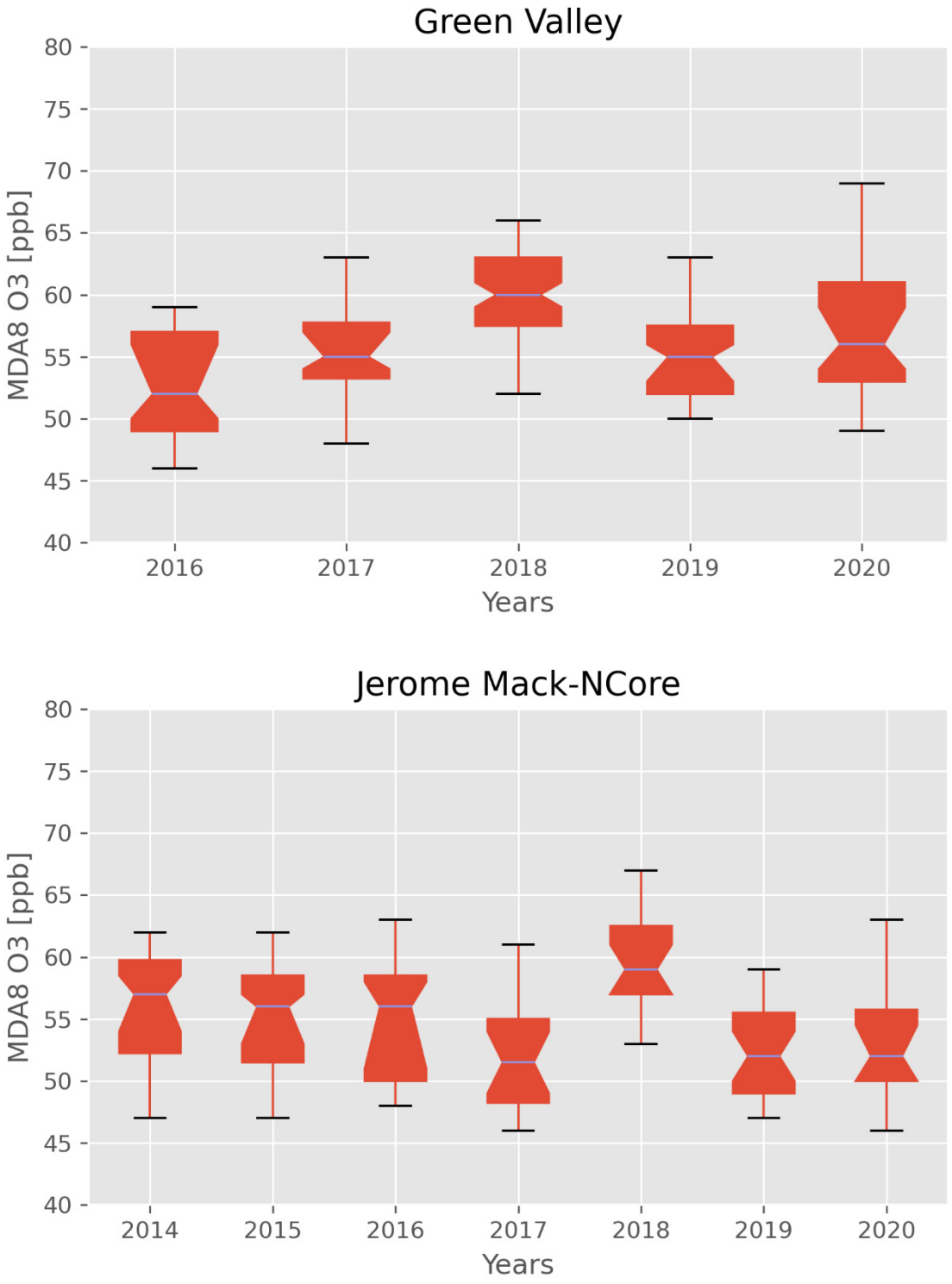

Figure G-2 (Cont.). Annual May distributions of MDA8 ozone at sites with exceptional events during May 2020. Notches denote 95th confidence interval of the median, boxes are 25th, 50th and 75th percentiles, and whiskers are 5th and 95th percentiles.

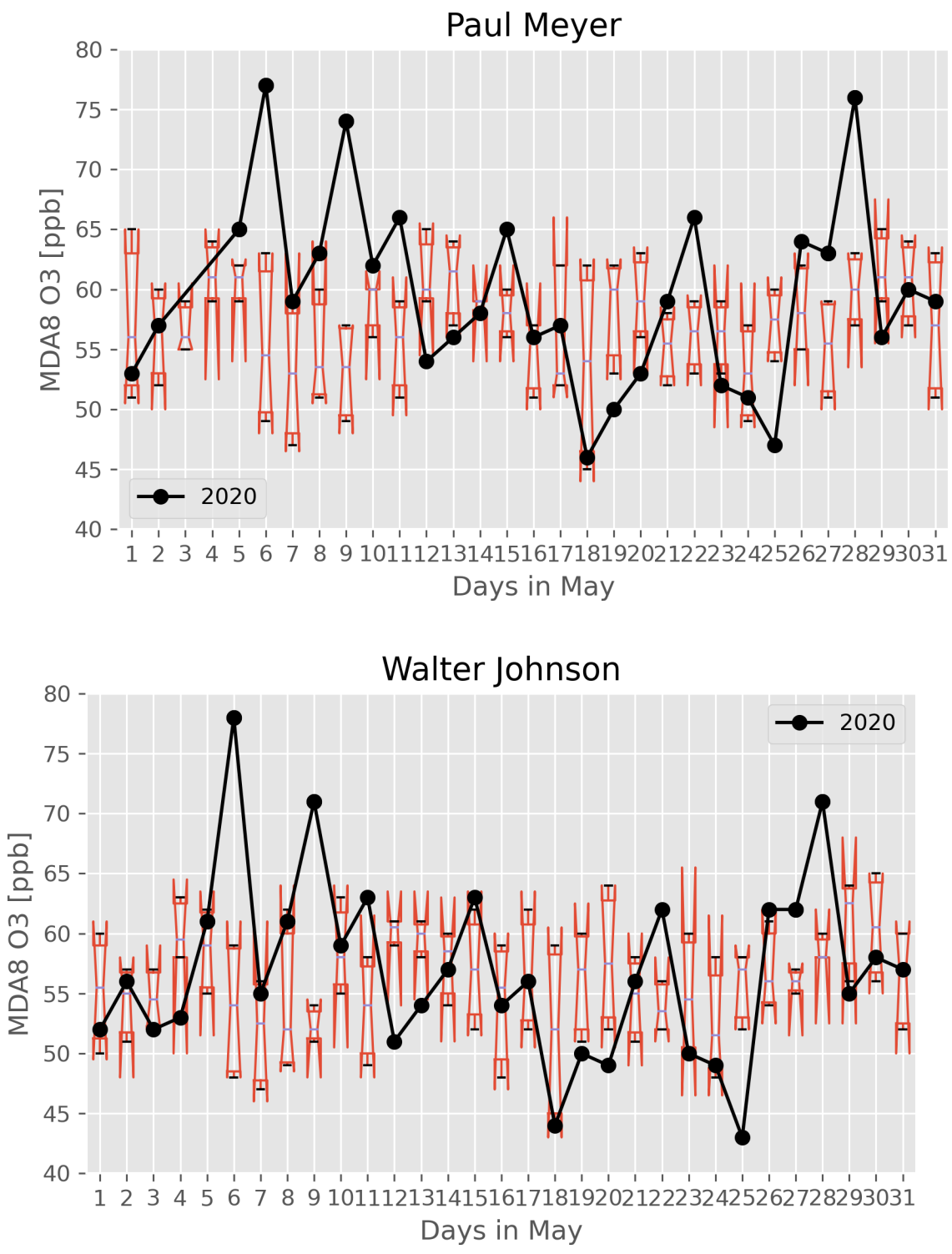

Figure G-3. Daily time series of 2014-2019 MDA8 ozone distributions and 2020 MDA8 ozone at each site with proposed exceptional event during May 2020. Notches denote 95th confidence interval of the median, boxes are 25th, 50th and 75th percentiles, and whiskers are 5th and 95th percentiles.

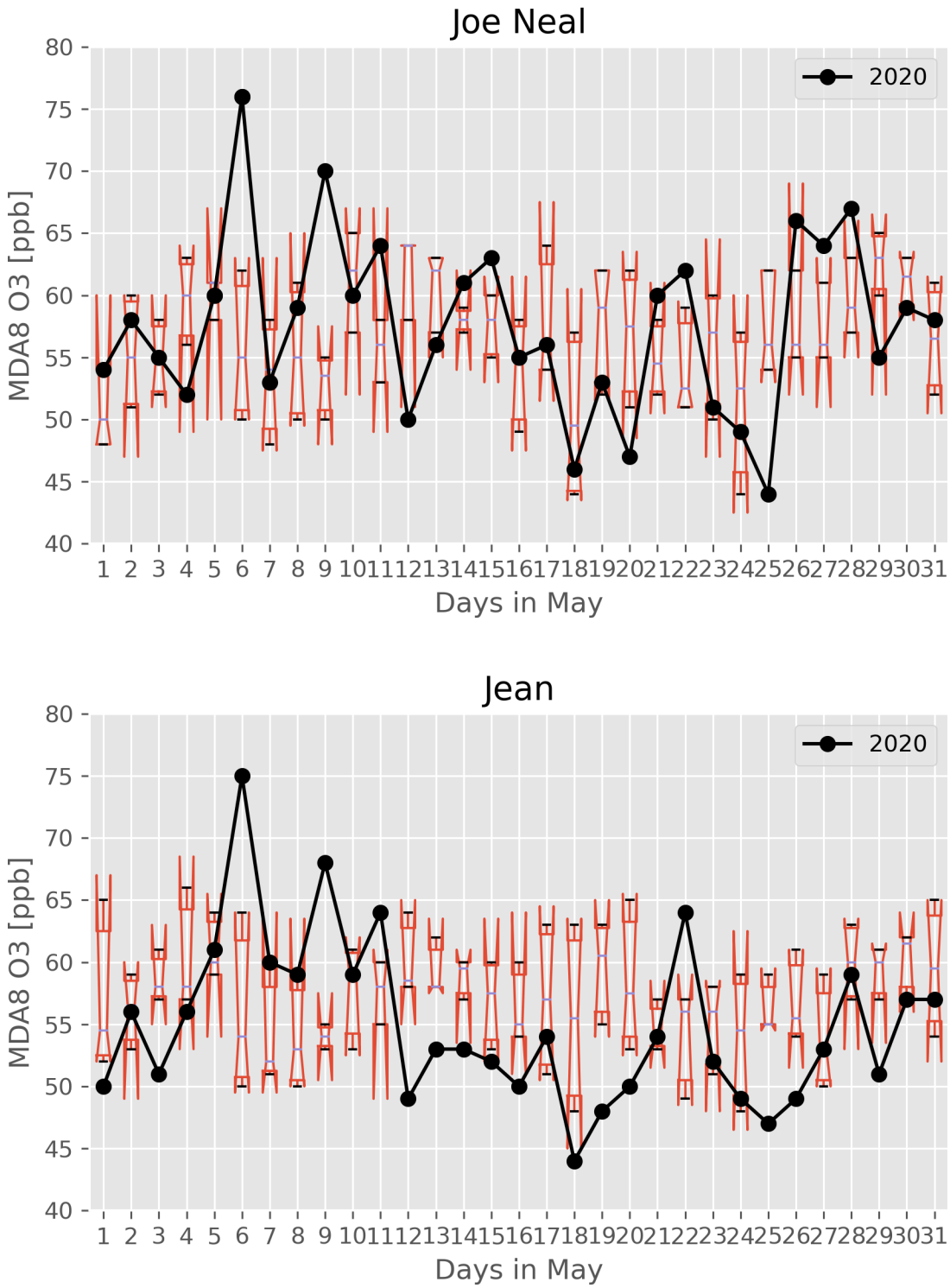

Figure G-3 (Cont.). Daily time series of 2014-2019 MDA8 ozone distributions and 2020 MDA8 ozone at each site with proposed exceptional event during May 2020. Notches denote 95th confidence interval of the median, boxes are 25th, 50th and 75th percentiles, and whiskers are 5th and 95th percentiles.

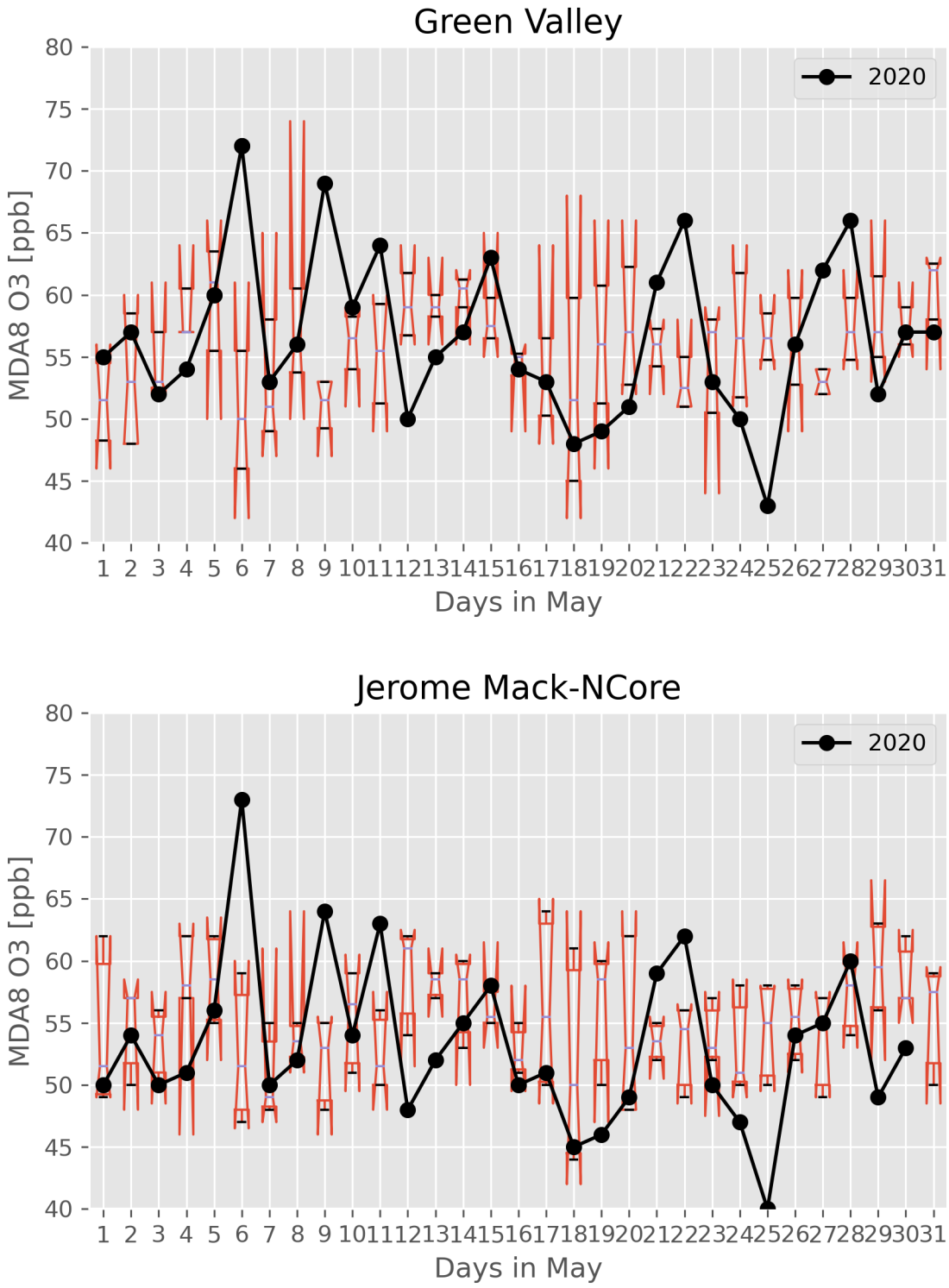

Figure G-3 (Cont.). Daily time series of 2014-2019 MDA8 ozone distributions and 2020 MDA8 ozone at each site with proposed exceptional event during May 2020. Notches denote 95th confidence interval of the median, boxes are 25th, 50th and 75th percentiles, and whiskers are 5th and 95th percentiles.

References

Clark County Department of Environment and Sustainability (2020) Revision to the Nevada State implementation plan for the 2015 ozone NAAQS: emissions inventory and emissions statement requirements. September. Available at https://files.clarkcountynv.gov/clarknv/Environmental%20Sustainability/SIP%20Related%20Documents/O3/20200901_2015_O3%20EI-ES_SIP_FINAL.pdf?t=1617690564073&t=1617690564073.

Kroll J.H., Heald C.L., Cappa C.D., Farmer D.K., Fry J.L., Murphy J.G., and Steiner A.L. (2020) The complex chemical effects of COVID-19 shutdowns on air quality. *Nature Chemistry*, 12(9), 777-779, doi: 10.1038/s41557-020-0535-z. Available at https://doi.org/10.1038/s41557-020-0535-z.

Parker H.A., Hasheminassab S., Crounse J.D., Roehl C.M., and Wennberg P.O. (2020) Impacts of traffic reductions associated with COVID-19 on Southern California air quality. Geophysical Research Letters, 47(23), e2020GL090164. Available at https://agupubs.onlinelibrary.wiley.com/doi/abs/10.1029/2020GL090164.

Venter Z.S., Aunan K., Chowdhury S., and Lelieveld J. (2020) COVID-19 lockdowns cause global air pollution declines. Proceedings of the National Academy of Sciences, 117(32), 18984-18990, doi: 10.1073/pnas.2006853117. Available at https://www.pnas.org/content/pnas/117/32/18984.full.pdf.

Appendix H. Documentation of Public Comment Process

To be updated once the public comment period has concluded.